ELSEVIER

Journal of Physics and Chemistry of Solids 60 (1999) 625–629

JOURNAL OF PHYSICS AND CHEMISTRY OF SOLIDS

Transmission electron microscopy studies of $Pb(Zr_{0.99}Ti_{0.01})O_3$ single crystals

N. Menguy[a], C. Caranoni[a], B. Hilczer[b,*], K. Roleder[c], J. Dec[c]

[a]*Laboratory MATOP-CNRS, Faculty of Sciences St. Jerome, University of Aix Marseille III, Av. Normandie-Niemen, F-13397 Marseille Cedex 20, France*

[b]*Institute of Molecular Physics, Polish Academy of Sciences, Smoluchowskiego 17, PL-60179 Poznań, Poland*

[c]*Institute of Physics, Silesian University, Uniwersytecka 4, PL-40007 Katowice, Poland*

Received 31 March 1998; received in revised form 5 August 1998; accepted 14 October 1998

Abstract

Room temperature HREM studies of $Pb(Zr_{0.99}Ti_{0.01})O_3$ single crystals revealed the presence of antiferroelectric alignment of the dipole moments along the $\langle 110\rangle_c$ similar to that observed in $PbZrO_3$. In the case of low Ti-content lead zirconate–lead titanate crystals we found, however, diffusseness of the 1/4 110 superlattice reflections along the $\langle 110\rangle_c$ indicating a local disorder in the lead sublattice. The walls between 60° domains were observed in $\langle 111\rangle_c$ and $\langle 110\rangle_c$ zone axis HREM images. Moreover, diffuse scattering along the $\langle 110\rangle_c$ direction was observed in the paraelectric phase (at 575 K) and related to the existence of nanosize polar clusters or pretransitional disorder.

Keywords: C. Electron microscopy; Lead zirconate–titanate

1. Introduction

Lead zirconate–titanate $Pb(Zr_{1-x}Ti_x)O_3$, further denoted as PZT, owing to its technological importance and a complex phase diagram [1–6] is still a focus of attention among physicist and material science researches. Nonlinear features, relaxor behaviour of La-modified PZT [7–11] and impurity-induced incommensurations in La, Nb and Sn-modified PZT [12–16] make the material interesting for investigations.

PZT with high Zr-content is antiferroelectric at room temperature and recently a revised phase diagram of this material has been published by Viehland [5]. In his transmission electron microscope (TEM) studies performed systematically in a wide temperature range on series of $Pb(Zr_{1-x}Ti_x)O_3$ (for $0 \le x \le 0.2$) Viehland found a local order in the rotation of oxygen octahedra in the high temperature paraelectric phase. Moreover, the pseudo-cubic $1/2\langle 110\rangle_c$ reflections were observed for PZT of $0 \le x \le 0.05$ and interpreted as a local ordering of oxygen octahedra tilts with tetragonal symmetry existing within the global rhombohedral structure owing to the long range order of Zr and Ti ion displacements along $\langle 111\rangle_c$ directions. The author related the ordered structure to nanosized (~10 nm) domain regions which may be associated with the roto-strictive coupling of the oxygen rotations to the dielectric polarization.

Transmission electron microscope studies of $PbZrO_3$ single crystals at room temperature and in the intermediate phase were performed by Tanaka et al. [17]. The authors observed 90° and 60° domain configurations and, in specific conditions, also 180° domains in the antiferroelectric phase of the crystals. The antiferroelectric phase of $PbZrO_3$ has an orthorhombic structure (Pbam space group) [6,18–21] with lattice parameters: $a_o = 0.5889(3)$ nm, $b_o = 1.1784(4)$ nm and $c_o = 0.8226(2)$ nm [21] ($a_o = \sqrt{2}a_c$, $b_o = \sqrt{2}a_c$, and $c_o = 2a_c$, where a_c denotes the lattice parameter of the cubic paraelectric phase).

The purpose of our study was to investigate the nanostructure and antiferroelectric domain structure of $Pb(Zr_{0.99}Ti_{0.01})O_3$ single crystal and to relate the structure to the displacement vector of the orthorhombic phase.

* Corresponding author. Tel.: +4861-861-2340.

E-mail address: bhilczer@ifmpan.poznan.pl (B. Hilczer)

0022-3697/99/$ - see front matter
PII: S0022-3697(98)00326-6

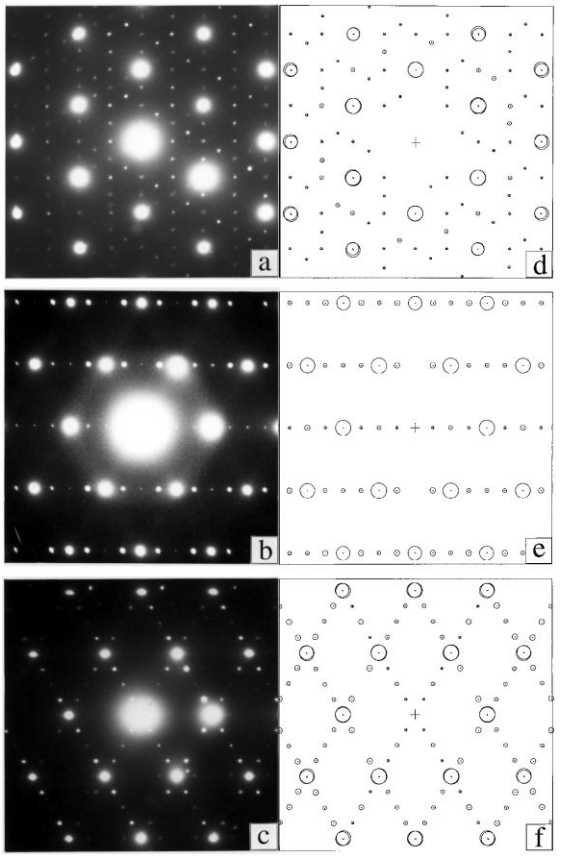

Fig. 1. (a), (b), (c): ⟨111⟩ zone axis SADP and corresponding simulated diffraction patterns (d), (e), (f) obtained from the structural data for pure $PbZrO_3$.

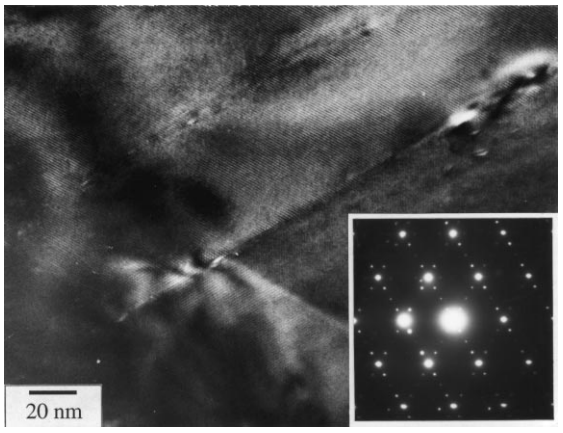

Fig. 2. Dark field image along a $\langle 111\rangle_c$ axis (exactly a $[201]_o$ axis) obtained by selecting a fundamental reflection with several superstructure reflections. Two sets of fringes with a spacing of 1.17 nm are visible perpendicularly to the direction where the superstructure reflections are lying (see the corresponding diffraction pattern shown in insert). A third set of vertical fringes is slightly visible and correspond to a third antifferroelectric domain.

2. Experimental

$Pb(Zr_{0.99}Ti_{0.01})O_3$ single crystals were grown by the flux method. A proper mixture of $PbZrO_3$, $PbTiO_3$, PbO and B_2O_3 was used and the soaking process was carried out in a Pt-crucible at the temperature of 1350 K for 4 hrs. The melt was cooled down to 1200 K at a rate of 9 K/hr with a constant temperature gradient along the axis of the crucible. At the temperature of 1200 K the contents of the crucible was poured out and slowly cooled down to the room temperature. The crystals were washed in an aqueous solution of glacial acetic acid. Transparent, light-grey crystals in the form of thin rectangular plates of several mm in size were obtained. The Ti-ion content in the crystal was determined in mole percentage by using the X-ray microanalysis technique. As the ratio of the counts of the Pb and Ti ions to the analytical dispersion rarely exceeds the critical Fisher value, the crystals could be regarded as chemically homogeneous in the scale of spatial resolution of the method used, i.e., of a few cubic μm.

For transmission electron microscopy (TEM) studies, the crystal was crushed in an agate mortar and deposited on holey carbon films. TEM experiments, high resolution electron microscopy (HREM) and selected area diffraction pattern (SADP) studies, were carried out on a Jeol 200CX transmission electron microscope at room temperature at an accelerating voltage of 200 kV. High temperature TEM experiments were performed using a double-tilt heating specimen holder on a Jeol 3010 transmission electron microscope at accelerating voltage of 300 kV.

3. Results

Figs. 1a, b and c show three $\langle 111\rangle_c$ zone axis SADP obtained from fragments of $Pb(Zr_{0.99}Ti_{0.01})O_3$ single crystal. Well defined 1/4 001_c superstructure reflections are visible along the $\langle 110\rangle_c$ directions. In order to interpret the observed difference regarding the positions of the superstructure reflections in various reciprocal planes, diffraction pattern simulations were made from the structural data and model proposed by Glazer for pure $PbZrO_3$ [6] using the EMS software of Stadelmann [22]. The experimental SADP of $Pb(Zr_{0.99}Ti_{0.01})O_3$ (Figs.1a, b and c) and simulated SADP of pure $PbZrO_3$ (Figs.1d, e and f appear to be in good agreement. This indicates that the low Ti-concentration does not induce a major structural difference in the $PbZrO_3$ phase. Moreover, it can be observed that each of the SADP shown in Figs.1a and c results from a simultaneous diffraction of the electron beam by two antiferroelectric domains, since simulated SADP shown in Figs. 1d and f were obtained by taking into account a superposition of two diffraction patterns. The superstructure reflections observed in $PbZrO_3$ and $Pb(Zr_{0.99}Ti_{0.01})O_3$ are because of the condensation of (1/2 1/2 0) $(\pi/a)\Sigma_3$ soft mode containing antiparallel displacements of the Pb-cations in {001} plane [21].

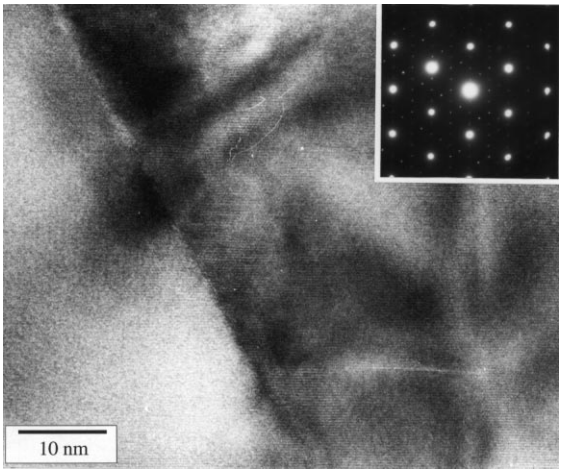

Fig. 3. High magnification image obtained with the electron beam parallel to a $\langle 111\rangle_c$ axis (exactly a $[011]_o$ axis). Along this direction, only the domain wall, a $(110)_c$ plane, is visible.

The real domain structure of $Pb(Zr_{0.99}Ti_{0.01})O_3$ single crystals is, generally speaking, rather complex. At room temperature the antiferroelectric perovskite structure of the crystal is the same as for $PbZrO_3$ crystals with the orthorhombic Pbam space group [6,20,21]. The antiparallel polarization in the crystals of the orthorhombic symmetry can take the direction of $\langle 110\rangle_c$ type, and the $\{100\}_c$ and $\{110\}_c$ planes can be the 90° and 60° domain walls, respectively [17,23]. Fig. 2 shows a dark field image of $Pb(Zr_{0.99}Ti_{0.01})O_3$ fragment obtained along a $\langle 111\rangle_c$ pseudocubic direction ($[201]_o$ orthorhombic direction) by selecting a fundamental 220_c reflection with several superstructure reflections. The insert in Fig. 2 shows that the corresponding diffraction pattern is the same as the one shown in Fig. 1c. Two sets of fringes perpendicular to the $\langle 011\rangle_c$ directions, with the periodicity of about 1.18 nm visible in the picture, belong to 60° antiferroelectric domains separated by domain walls. The two 60° domains relate to each other by the symmetry plane $\{110\}_c$ of the pseudo-cubic structure.

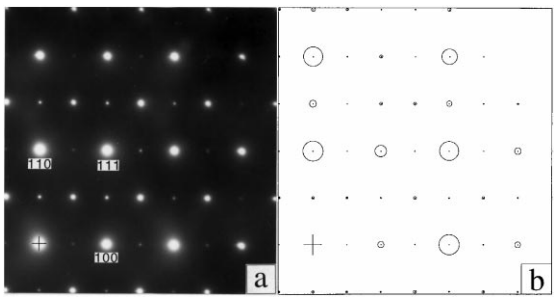

Fig. 4. $\langle 110\rangle_c$ zone axis SADP. 1/2 111, 1/2 110 and 1/2 100 reflections are visible. It can be deduced from simulated diffraction pattern related to pure $PbZrO_3$ that, in the orthorhombic axes, the zone axis is $[100]_o$.

Further, the domain boundary, as having a defined thickness owing to the loss of the periodicity, induces a local strain field which results in the variation of contrast. When the incident beam is not perfectly parallel to the domain wall a phase shift in the beam wave function is induced. The resulting contrast consists of alternating dark and bright fringes parallel to the intersection of the wall with the crystal surface (see Fig. 2). Different origin of the ferroic domain contrast was discussed earlier by several authors [17,24,25]. High magnification image obtained with the electron beam parallel to another $\langle 111\rangle_c$, namely, the $[011]_o$ orthorhombic direction, is shown in Fig. 3. Only the domain wall between 60° domains is visible in the $\{110\}_c$ planes. Moreover, a change in contrast of bright and dark fringes can be seen, parallel to the intersection of the wall and the sample surface. This contrast variation results from the fact that the domain wall is not perfectly parallel to the electron beam [24]. Fig. 4 shows a $\langle 110\rangle_c$ zone axis SADP with well resolved 1/2 111, 1/2 110 and 1/2 100 superstructure reflections. The 1/2 111 reflections (F-spots termed by Viehland [5]) are related to the condensation of the Γ_{25} soft mode resulting in a complex oxygen rotation around the $\langle 110\rangle_c$ direction, which stabilize the oxygen framework of the orthorhombic structure.

The diffraction pattern simulation based on the $PbZrO_3$ structure shows that the incident electron beam in the $\langle 111\rangle_c$ pseudocubic direction corresponds to the $[100]_o$ orthorhombic zone axis. Fig. 5a shows HREM image obtained with the incident electron beam along the $\langle 110\rangle_c$ direction. The picture exhibits sets of fringes parallel to the $\langle 111\rangle_c$ and $\langle 100\rangle_c$ directions, as illustrated in Fig. 5b. The contrast is owing to the existence of domain walls which are tilted with respect to the electron beam. The sets of fringes parallel to the $\langle 111\rangle_c$ and $\langle 100\rangle_c$ directions correspond to $\{110\}_c$ and $\{100\}_c$ domain walls, respectively. Fig. 6 shows the $[001]_o$ zone axis SADP and a corresponding simulated diffraction pattern. The reflections of 1/2 110 are visible in two perpendicular directions owing to simultaneous diffraction of the electron beam by two neighboring antiferroelectric domains rotated by 90° with respect to each other (90° domains). This observation is similar to the one reported by Tanaka for $PbZrO_3$ [17]. The superlattice reflections along $\langle 110\rangle$ direction point to the quadrupling of the paraelectric cubic perovskite unit cell caused by the Σ_3 soft mode which leads to antipolar displacements of Pb-cations in the antiferroelectric, orthorhombic state. It should be noted that the 1/4 110 spots are circular whereas the 1/4 110 spots are rather diffused in the $\langle 110\rangle$ directions. This may be attributed to the disorder in the Pb-cation displacements. Our hypothesis seems to be corroborated by the results reported for $PbZrO_3$ by Viehland [5] who observed very sharp 1/4 110 superstructure reflections at high temperature (443 K); on cooling these spots became more diffuse. This diffuseness occurs, most probably, by the onset of some local static disorder.

Fig. 7 shows a $[001]_o$ zone axis SADP obtained from a fragment of $Pb(Zr_{0.99}Ti_{0.01})O_3$ single crystal at 575 K.

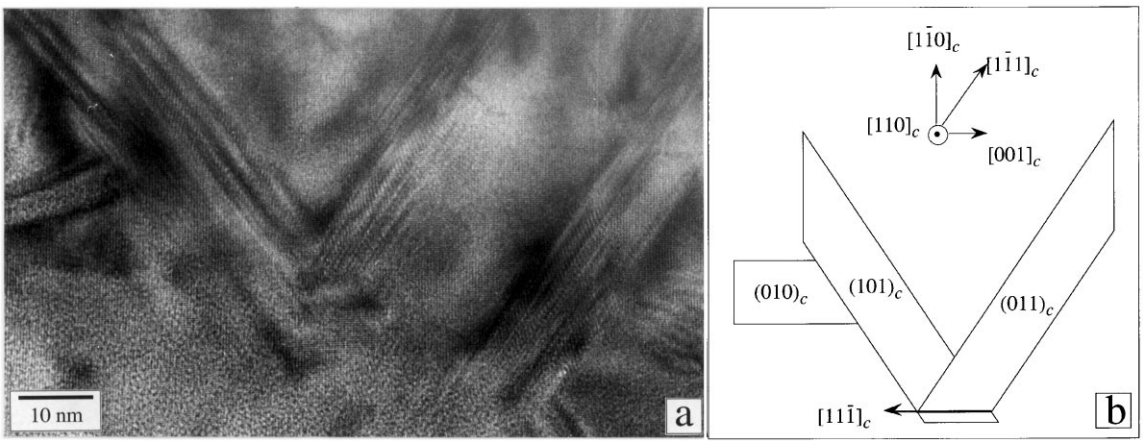

Fig. 5. (a) HREM image of $Pb(Zr_{0.99}Ti_{0.01})O_3$ with the incident electron beam in the$\langle 110\rangle_c$ pseudocubic direction. The contrast results mainly from the existence of inclined $\{110\}_c$ domain walls with respect to the foil orientation as shown in (b). All crystallographic directions are related to the pseudo-cubic axes.

Diffuse scattering is clearly visible along the $\langle 110\rangle_c$ directions of the reciprocal space. This behavior seems to be very similar to that observed for $Pb(Sc_{0.5}Ta_{0.5})O_3$ exhibiting ferroelectric relaxor properties [26,27]. In the case of $Pb(Zr_{0.99}Ti_{0.01})O_3$ single crystals the diffuse scattering can be seen as precursor state of the antiferroelectric phase.

4. Conclusion

The results of our electron microscope studies show that the room temperature antiferroelectric domain structure of $Pb(Zr_{0.99}Ti_{0.01})O_3$ single crystals is the same as the one reported earlier for $PbZrO_3$ at room temperature [5,17]. The 90° domains occurring was observed in two perpendicular sets of 1/4 110 reflections in the $[001]_o$ zone axis SADP. In addition, walls between 60° domains were evidenced in $\langle 111\rangle_c$ and $\langle 110\rangle_c$ zone axis HREM images.

Condensation of the antiferroelectric Σ_3 mode could be seen in properly selected area diffraction patterns as the 1/4 110 superlattice reflections related to antiparallel alignment of the dipole moments along the $\langle 110\rangle_c$ direction. Moreover, weak superlattice reflections of 1/2 111 type observed in the $\langle 110\rangle_c$ zone axis SADP confirmed the existence of Γ_{25} oxygen rotation mode.

This is in accord with the phase diagram of $PbZr_{1-x}Ti_xO_3$ with $x < 0.2$ (high zirconium content) revised and reported recently by Viehland [5]. In our opinion the diffuse scattering observed at the high temperature, in the paraelectric phase of the $Pb(Zr_{0.99}Ti_{0.01})O_3$ single crystal (Fig. 7), is related to the existence of nano-sized polar clusters or a pretransitional ordering. We also found 1/4 110 superlattice reflections, related to the Pb-cation displacements in the $(001)_c$ plane, to be diffused along the $\langle 110\rangle_c$ directions at room temperature. It seems that this behavior reflects a local disorder in the lead sublattice which mostly probably is an intrinsic feature of the studied crystal in the antiferroelectric phase.

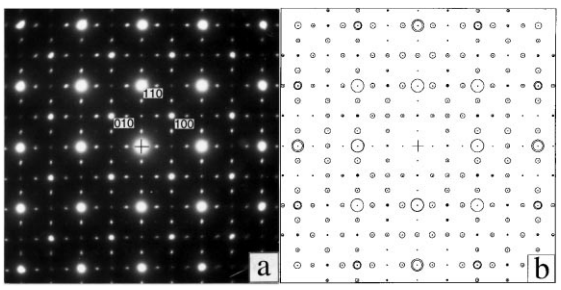

Fig. 6. (a) $[001]_o$ zone axis SADP and corresponding simulated diffraction pattern (b). The diffuseness of the 1/4 110 reflections on the experimental SADP has to be noticed.

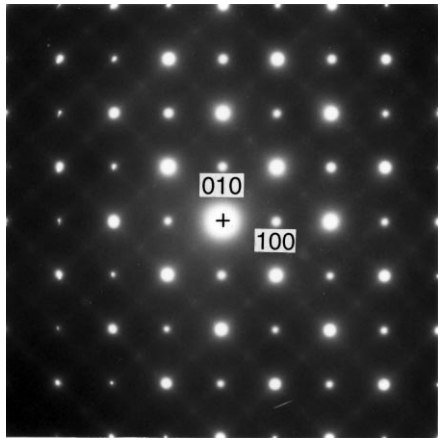

Fig. 7. $[001]_o$ zone axis SADP at about 575 K. 1/2 110 and 1/4 110 reflections which were present at room temperature are no longer visible and a diffuse scattering along the $\langle 110\rangle_c$ directions can be seen.

References

[1] D. Berlincourt, IEEE Trans. Sonics Ultrason. Su. 13 (1966) 113.
[2] E. Sawaguchi, J. Phys. Soc. Jpn. 8 (1953) 615.
[3] O.E. Fesenko, V.V. Emrekin, V.G. Smotrakov, S.M. Zaitsev, Sov. Phys. Solid State 28 (1986) 181.
[4] H. Banno, in, The Encyclopedia of advanced Materials (1994) p. 2017.
[5] D. Viehland, Phys. Rev. B 52 (1995) 778.
[6] A.M. Glazer, K. Roleder, J. Dec, Acta Cryst. B 49 (1993) 846.
[7] C.A. Randall, D.J. Barber, R.W. Whatmore, J. of Microscopy 145 (3) (1987) 275.
[8] D. Viehland, S.J. Jang, L.E. Cross, M. Wuttig, J. Appl. Phys. 69 (1991) 6595.
[9] C.A. Randall, G.A. Rosetti, W. Cao, Ferroelectrics 150 (1993) 163.
[10] A. Krumins, T. Shiozaki, S. Koizumi, Jpn. J. Appl. Phys. 33 (1994) 4940.
[11] F. Fang, H. Gui, X. Zhang, Ferroelectrics 175 (1996) 233.
[12] Z. Xu, D. Viehland, P. Yang, D.A. Payne, J. Appl. Phys. 74 (1993) 3406.
[13] Z. Xu, D. Viehland, D.A. Payne, J. Mat. Res. 10 (1995) 453.
[14] D. Forst, D. Viehland, J. Appl. Phys. 76 (1994) 5891.
[15] X.D. Dai, D. Viehland, Ferroelectrics 158 (1994) 375.
[16] D. Viehland, J.F. Li, X. Dai, Z. Xu, J. Phys. Chem. Sol. 57 (1996) 1545.
[17] M. Tanaka, R. Saito, K. Tsuzuki, Jpn. J. Appl. Phys. 21 (1982) 291.
[18] E. Sawaguchi, H. Maniwa, S. Hoshino, Phys. Rev. 83 (1951) 1078.
[19] F. Jona, G. Shirane, F. Mazzi, R. Pepinksky, Phys. Rev. 105 (1957) 847.
[20] M. Tanaka, R. Saito, K. Tsuzuki, J. Phys. Soc. Jpn. 51 (1982) 2635.
[21] H. Fujishita, S. Hosino, J. Phys. Soc. Jpn. 226 (1984) 2635.
[22] P.A. Stadelmann, Ultramicroscopy 21 (1987) 131.
[23] J. Dec, Crystal Res. Technol. 18 (1983) 195.
[24] F. Tsai, V. Khiznichenko, J.M. Cowley, Ultramicroscopy 45 (1992) 55.
[25] E. Snocck, L. Normand, A. Thorel, C. Roucau, Phase Transitions 46 (1994) 77.
[26] K.Z. Baba-Kishi, D.J. Barber, J. Appl. Cryst. 23 (1990) 43.
[27] K.Z. Baba-Kishi, G. Gressey, R.J. Cernik, J. Appl. Cryst. 25 (1992) 477.